Bull. Chem. Soc. Jpn., **68**, 1136—1144(1995)

Crystal Structures and Electrical Resistivities of Three-Component Organic Conductors: $(BEDT\text{-}TTF)_2MM'(SCN)_4$ [M=K, Rb, Cs; M'=Co, Zn, Cd]

Hatsumi Mori,* Shoji Tanaka, Takehiko Mori,† and Yusei Maruyama††

International Superconductivity Technology Center, Shinonome, Tokyo 135

†Department of Organic and Polymeric Materials, Tokyo Institute of Technology, O-okayama, Tokyo 152

††Institute for Molecular Science, Okazaki 444

(Received November 10, 1994)

New three-component organic conductors, $(BEDT\text{-}TTF)_2MM'(SCN)_4$ [M=K, Rb, Cs; M'=Co, Zn, Cd], are prepared. The crystal structure analyses of α-$ET_2CsCo(SCN)_4$, $ETZn(SCN)_3$, α-$ET_2RbZn(SCN)_4$, α-$ET_2CsZn(SCN)_4$, α-$ETCd_{0.66}(SCN)_2$, and $ET_2CsCd(SCN)_4$ are carried out. Most of salts have the α-type donor arrangement and the polymer sheet like $[\cdots M'^{2+}\cdots(SCN)^-\cdots M^+\cdots]$ in a thick anion layer. Especially α-$(BEDT\text{-}TTF)_2CsM'(SCN)_4$ [M'=Co and Zn] are metallic down to 20 K.

Organic conductors with three-component system as $(BEDT\text{-}TTF)_2MHg(SCN)_4$ [BEDT-TTF=bis(ethylenedithio)tetrathiafulvalene, M=Li, Na, K, (Tl), NH_4, Rb, and Cs (r(ionic radius)=0.7—1.7 Å)[1)]] which vary from semiconductors to superconductors have been obtained.[2)] It is interesting that the third component, the cation, controls the donor arrangement, which determines the electronic state of the salts. Since the radii of K^+, Tl^+, NH_4^+, and Rb^+ are close, these salts are isostructural. The physical properties are, however, quite different; the K^+, Tl^+, and Rb^+ salts are metallic down to 0.6 K with the anomaly around 10 K due to the SDW (Spin Density Wave) transition.[2f,3)] These salts have two-dimensional closed Fermi surface and one-dimensional open one. When the latter one is nested, the SDW transition occurs. On the other hand, the NH_4 salt shows superconducting transition at 0.8 K.[2e,4)] Since the unit cell volume increases in the order of the K salt (1988 Å^3) <the Tl salt (1989 Å^3) <the NH_4 salt (2006 Å^3) <the Rb salt (2010 Å^3),[5)] the NH_4 salt is not exceptional. The reason why the SDW instability was not observed only for the NH_4 salt might be related to hydrogen contacts. The Li and Cs salts have different crystal structures from the isostructural four salts and the donor arrangements are β- and α''-type respectively. β-$(BEDT\text{-}TTF)_3Li_{0.5}Hg(SCN)_4(H_2O)_2$ and α''-$(BEDT\text{-}TTF)_2CsHg(SCN)_4$ are metallic down to 170 and 210 K.

In order to develop this system, $MM'(SCN)_n$ [M=K, Rb, Cs; M'=Co, Zn, Cd] salts based upon BEDT-TTF have been investigated and some organic conductors with two- or three-component system have been obtained. For the Co salts, whether the localized spin of Co^{2+} and the itinerant spin of BEDT-TTF interact or not is interesting. In this paper the crystal structures of α-$(BEDT\text{-}TTF)_2CsCo(SCN)_4$, $(BEDT\text{-}TTF)Zn(SCN)_3$, α-$(BEDT\text{-}TTF)_2RbZn(SCN)_4$, α-$(BEDT\text{-}TTF)_2CsZn(SCN)_4$, α-$(BEDT\text{-}TTF)Cd_{0.66}(SCN)_2$, and $(BEDT\text{-}TTF)_2CsCd(SCN)_4$ and the electrical resistivities of the new three-component salts are described compared with the $MHg(SCM)_4$ system.

Experimental

Single crystals were obtained by oxidation of BEDT-TTF with using $M'(SCN)_2$ [M'=Co, Zn, and Cd], MSCN (M=Li, Na, K, NH_4, Rb, and Cs), and 18-crown-6 in 1,1,2-trichloroethane and ethanol. The preparations, crystal shapes and electrical resistivities of obtained $MM'(SCN)_n$ complexes are shown in Table 1 and crystallographic data are in Table 2. The complete F_o-F_c data are deposited as Document No. 68014 at the Office of the Editor of Bull. Chem. Soc. Jpn. The crystal reflection data were collected on Rigaku 5R diffractometer [Mo $K\alpha$ (λ=0.71073 Å), $2\theta<60^\circ$] or Nonius diffractometer [Cu $K\alpha$ (λ=1.54184 Å), $2\theta<140^\circ$] corrected for usual Lorentz and polarization effects for all salts and absorption for α-$(BEDT\text{-}TTF)_2CsM'(SCN)_4$ [M'=Co and Zn]. The crystal structures were solved by the direct method (Shelex 86[6)]) and refined by the least-squares procedure. The temperature factor were refined anisotropically for the non-hydrogen atoms. EDX (Energy Dispersion X-ray spectroscopy) measurements were carried out on JEOL JSM-5400LV operated at 20 kV in order to observe contained elements larger than Na and a stoichiometry of a salt. The electrical resistivities were measured by applying ac current (50 Hz) with gold paste as a contact. A pressure cell of a clamp type was used with an oil (Daphne #7373) as a pressure medium.

Table 1. Preparations, Crystal Shapes, and Electrical Resistivities of $MM'(SCN)_n$ Complexes

Preparation[a]	Complexes	Crystal shape	Electrical resistivity
BEDT-TTF+LiSCN+$Co(SCN)_2$+18-C-6 in TCE+EtOH	—	Black plate	—
NaSCN	$(et)_2Co(SCN)_4$[c]	Black plate	σ_{RT}=1 S cm^{-1}, E_a=0.06 eV
KSCN	$(et)_2$**K**$Co(SCN)_4$[c]	Black plate	σ_{RT}=6 S cm^{-1}, T_{MI}=300 K, E_a=0.05 eV
NH_4SCN	—	Flake	—
RbSCN	$(et)_2$**Rb**$Co(SCN)_4$[c]	Black needle	σ_{RT}=5 S cm^{-1}, E_a=0.11 eV
CsSCN	α-$(et)_2$**Cs**$Co(SCN)_4$[b]	Black needle	σ_{RT}=14 S cm^{-1}, T_{MI}=20 K
BEDT-TTF+LiSCN+$Zn(SCN)_2$+18-C-6 in TCE+EtOH	—	Black plate	—
NaSCN	—	—	—
KSCN	$(et)_2$**K**$Zn(SCN)_4$[c]	Black needle	σ_{RT}=28 S cm^{-1}, E_a=0.07 eV
NH_4SCN	$(et)Zn(SCN)_3$[b]	Black plate	ρ_{RT}=180 Ω cm, E_a=0.18 eV
RbSCN	α-$(et)_2$**Rb**$Zn(SCN)_4$[b]	Black needle	σ_{RT}=12 S cm^{-1}, T_{MI}<180 K
CsSCN	α-$(et)_2$**Cs**$Zn(SCN)_4$[b]	Black needle	σ_{RT}=110 S cm^{-1}, T_{MI}=20 K
BEDT-TTF+LiSCN+$Cd(SCN)_2$+18-C-6 in TCE+EtOH	—	Black needle	ρ_{RT}=6 Ω cm, E_a=0.10 eV
NaSCN	—	Flake	—
KSCN	$(et)_2$**K**$Cd(SCN)_4$[c]	Black plate	—
NH_4SCN	α-$(et)Cd_{0.66}(SCN)_2$[b]	Black plate	σ_{RT}=4 S cm^{-1}, E_a=0.11 eV
RbSCN	—	Black plate	ρ_{RT}=5 Ω cm, E_a=0.14 eV
CsSCN	$(et)_2$**Cs**$Cd(SCN)_4$[b]	Black plate	σ_{RT}=10 S cm^{-1}, E_a=0.02 eV

a) et=BEDT-TTF, 18-C-6=18-Crown-6, TCE=1,1,2-trichloroethane. b) The stoichiometries are determined by EDX measurements and crystal structure analyses. c) The stoichiometries are determined by EDX measurements.

Table 2. The Lattice Parameters of $MM'(SCN)_n$ Complexes (et=BEDT-TTF)

	α-$(et)_2CsCo(SCN)_4$	$(et)Zn(SCN)_3$	α-$(et)_2RbZn(SCN)_4$	α-$(et)_2CsZn(SCN)_4$	α-$(et)Cd_{0.66}(SCN)_2$	$(et)_2CsCd(SCN)_4$
Chemical formula	$CsCoS_{20}N_4C_{24}H_{16}$	$ZnS_{11}N_3C_{13}H_8$	$RbZnS_{20}N_4C_{24}H_{16}$	$CsZnS_{20}N_4S_{24}H_{16}$	$Cd_{0.66}S_{10}N_2C_{12}H_8$	$CsCdS_{20}N_4C_{24}H_{16}$
Fw	1193.6	624.3	1152.6	1200.0	575.1	1247.0
System	Orthorhmbic	Triclinic	Monoclinic	Orthorhmbic	Monoclinic	Triclinic
Space group	$I222$	$P\bar{1}$	$C2$	$I222$	$C2/c$	$P\bar{1}$
a/Å	9.804(4)	13.210(4)	45.480(33)	9.816(4)	41.469(10)	8.982(2)
b/Å	43.416(3)	15.087(6)	10.177(9)	43.443(4)	4.277(10)	20.803(5)
c/Å	4.873(4)	5.925(2)	4.649(2)	4.870(4)	11.542(8)	5.794(2)
α/°	90	92.17(3)	90	90	90	90.51(2)
β/°	90	96.35(3)	107.86(4)	90	101.88(5)	102.92(2)
γ/°	90	108.79(3)	90	90	90	99.65(2)
V/Å^3	2074(3)	1107.5(7)	2048.1	2077(2)	2003(5)	1039.0(5)
Z	2	2	2	2	4	1
R	0.038	0.053	0.13	0.12	0.074	0.12
D_c	1.91	1.87	1.87	1.92	1.91	1.99
No. of ref.	757	2235	1268	728	1377	1450
	$\|I_o\|>3\sigma\|I_o\|$	$\|F_o\|>3\sigma\|F_o\|$	$\|F_o\|>3\sigma\|F_o\|$	$\|I_o\|>3\sigma\|I_o\|$	$\|F_o\|>3\sigma\|F_o\|$	$\|F_o\|>3\sigma\|F_o\|$
$2\theta_{max}$/°	60	60	140	60	60	60
λ/Å	0.71073	0.71073	1.54184	0.71073	0.71073	0.71073

Results and Discussion

As shown in Table 1, metallic behaviors are observed for the samples of α-(BEDT-TTF)$_2$CsCo(SCN)$_4$, α-(BEDT-TTF)$_2$RbZn(SCN)$_4$, and α-(BEDT-TTF)$_2$CsZn(SCN)$_4$. Figure 1 shows the temperature dependence of resistivity for α-(BEDT-TTF)$_2$CsZn(SCN)$_4$. At an ambient pressure the weak metallic behavior is observed down to 20 K and the distinct metal-insulator transition occurs below that temperature. When the same sample is pressurized to 5 kbar, the resistivity increases and the semiconducting behavior is observed even from room temperature. The same phenomena that the resistivity in the pressurized condition increases with lowering temperature is observed for (BEDT-TTF)$_5$Hg$_3$Br$_{11}$.[7] Since α-(BEDT-TTF)$_2$CsCo(SCN)$_4$ is isostructural to α-(BEDT-TTF)$_2$CsZn(SCN)$_4$, the temperature dependence of electrical resistivity at an ambient pressure for α-(BEDT-TTF)$_2$CsCo(SCN)$_4$ is similar though the conductivity (σ_{RT}=14 S cm^{-1}) is lower than that of α-(BEDT-TTF)$_2$CsZn(SCN)$_4$ (σ_{RT}=110 S cm^{-1}).

The crystal structure analyses were carried out for the underlined samples in Table 1. The atomic coordinates and equivalent isotropic thermal parameters are listed on Tables 3, 4, 5, 6, 7, and 8. Although most of the donor arrangement of three-component salts are α-type except for (BEDT-TTF)$_2$CsCd(SCN)$_4$, the crystal system varies from monoclinic ($C2$ and $C2/c$) to orthorhombic ($I222$). These symmetries are higher than α-(BEDT-TTF)$_2$MHg(SCN)$_4$ [M=K, NH$_4$, and Rb] whose crystal systems are triclinic[1b] and the lattice parameters in the stacking direction of these monoclinic and orthorhombic materials (4.3—4.9 Å) are half of the MHg(SCN)$_4$ system (9.9—10.0 Å), so that every BEDT-TTF stacks uniformly.

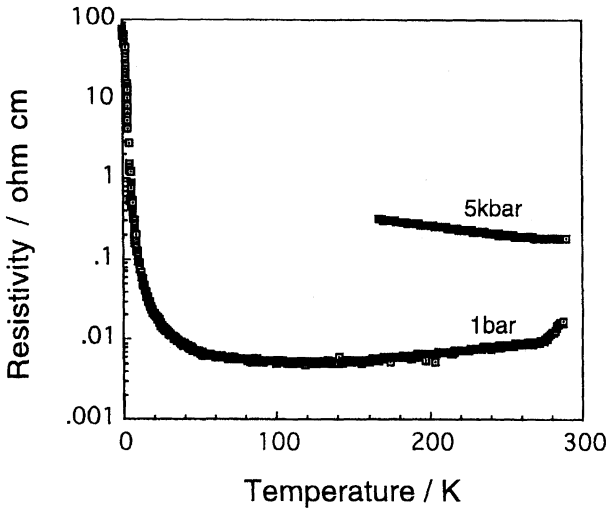

Fig. 1. Temperature dependence of electrical resistivity at 1 bar and 5 kbar for α-(BEDT-TTF)$_2$CsZn(SCN)$_4$.

The atomic parameters of α-(BEDT-TTF)$_2$CsM'(SCN)$_4$ [M'=Co and Zn] are in Tables 3 and 4 and the crystal structure and donor arrangement of α-(BEDT-TTF)$_2$CsCo(SCN)$_4$ are shown in Fig. 2. The BEDT-TTF molecule is on the two-fold axis, the Co^{2+} and Cs^+ are located on the cross point of three two-fold axes, and one SCN is on a general position. Therefore the crystallographically independent molecules are a half of BEDT-TTF, 1/4 of Co^{2+} and Cs^+, and one SCN. The distances of the central C=C and C–S are 1.37(1) and 1.732(6)—1.748(7) Å respectively, which suggests that the charges on BEDT-TTF are between

Table 3. Atomic Coordinates and Equivalent Isotropic Thermal Parameters of α-(BEDT-TTF)$_2$CsCo(SCN)$_4$

Atom	x	y	z	B_{eq}/Å^2
Co	0	0	0	4.2(1)
Cs	1/2	0	0	4.60(8)
S(1)	0.6434(3)	0.62656(5)	0.2817(7)	4.1(1)
S(3)	0.6178(3)	0.69402(5)	0.3115(7)	4.0(1)
S(5)	0.6189(3)	0.76831(5)	0.3175(6)	4.1(1)
S(7)	0.6437(3)	0.83544(5)	0.2836(6)	3.7(1)
C(1)	0.538(4)	0.5957(3)	0.402(7)	12(2)
C(3)	0.5535(8)	0.6579(2)	0.413(2)	3.5(6)
C(5)	1/2	0.7156(3)	1/2	3.3(6)
C(6)	1/2	0.7471(2)	1/2	3.3(6)
C(7)	0.5543(9)	0.8039(2)	0.416(2)	3.0(5)
C(9)	0.526(2)	0.8668(2)	0.349(3)	3.9(6)
S(50)	0.3221(3)	0.05457(6)	0.524(1)	5.7(2)
C(51)	0.202(1)	0.0373(2)	0.349(2)	3.6(5)
N(52)	0.120(1)	0.0249(2)	0.219(2)	4.8(5)
H(1)	0.51(5)	0.592(4)	0.26(4)	15(1)
H(2)	0.60(1)	0.581(3)	0.39(3)	7(5)
H(3)	0.576(9)	0.886(2)	0.32(2)	4(3)
H(4)	0.45(1)	0.865(2)	0.23(2)	3(3)

$\beta_{eq}=4/3(\sum_i \sum_j B_{ij}\ \boldsymbol{a}_i\cdot\boldsymbol{a}_j)$.

Table 4. Atomic Coordinates and Equivalent Isotropic Thermal Parameters of α-(BEDT-TTF)$_2$CsZn(SCN)$_4$

Atom	x	y	z	B_{eq}/Å^2
Zn	0	0	0	3.8(5)
Cs	1/2	0	0	3.6(3)
S(1)	0.643(1)	0.6268(2)	0.283(2)	3.7(5)
S(3)	0.619(1)	0.6955(3)	0.312(3)	4.1(6)
S(5)	0.619(1)	0.7692(2)	0.318(2)	3.5(4)
S(7)	0.642(1)	0.8360(2)	0.284(2)	3.3(5)
C(1)	0.540(5)	0.5940(8)	0.39(1)	7(3)
C(3)	0.554(3)	0.6583(7)	0.409(7)	3(2)
C(5)	1/2	0.713(1)	1/2	3(2)
C(6)	1/2	0.745(1)	1/2	5(3)
C(7)	0.554(4)	0.802(1)	0.419(8)	4(2)
C(9)	0.527(6)	0.8656(7)	0.348(9)	4(2)
S(50)	0.321(1)	0.0547(3)	0.528(4)	5.3(6)
C(51)	0.201(4)	0.0366(8)	0.349(9)	3(2)
N(52)	0.117(4)	0.0254(8)	0.231(8)	5(2)

$B_{eq}=4/3(\sum_i \sum_j B_{ij}\ \boldsymbol{a}_i\cdot\boldsymbol{a}_j)$.

Table 5. Atomic Coordinates ($\times 10^4$) and Equivalent Isotropic Thermal Parameters of α-(BEDT-TTF)-$Cd_{0.66}(SCN)_2$

Atom	x	y	z	B_{eq}/Å^2
Cd	0(0)	1901(5)	−2500(0)	4.6
S50	443(1)	3011(15)	2021(4)	10.0
C50	370(3)	2654(36)	543(11)	6.7
N50	312(3)	2454(40)	−466(11)	9.7
S1	3453(1)	5633(7)	−1748(2)	3.6
S2	3690(0)	9021(6)	1086(2)	3.5
S3	2786(0)	6086(7)	−1306(2)	3.6
S4	2974(0)	9112(7)	1025(2)	3.5
C1	3842(2)	7480(28)	−1095(7)	3.9
C2	3945(2)	6960(25)	225(7)	3.5
C3	3202(2)	6829(20)	−769(6)	2.6
C4	3290(2)	8121(20)	296(6)	2.4
C5	2656(2)	7545(21)	−58(6)	2.8
H1	384(2)	987(22)	−123(7)	6.7
H2	402(2)	660(22)	−146(7)	4.6
H3	395(2)	477(22)	40(7)	6.3
H4	416(2)	758(21)	45(7)	4.7

$B_{eq}=4/3(\sum_i\sum_j B_{ij}\ \boldsymbol{a}_i\cdot\boldsymbol{a}_j)$.

Table 6. Atomic Coordinates ($\times 10^4$) and Equivalent Isotropic Thermal Parameters of α-(BEDT-TTF)$_2$RbZn(SCN)$_4$

Atom	x	y	z	B_{eq}/Å^2
Zn	5000(0)	5885(8)	0(0)	3.5
Rb	5000(0)	856(8)	0(0)	5.2
S1	3738(2)	−543(10)	4096(24)	4.6
S2	3742(2)	2331(11)	8371(23)	4.8
S3	3063(2)	−307(11)	2390(23)	4.8
S4	3062(1)	2061(11)	5993(23)	4.7
S5	2315(2)	−318(11)	184(24)	4.7
S6	2317(2)	2085(11)	3681(22)	4.5
S7	1642(2)	−559(9)	−2148(22)	4.1
S8	1645(2)	2329(10)	2043(22)	4.3
C1	4060(8)	267(56)	6122(151)	11.9
C2	4085(12)	1115(136)	8497(187)	17.1
C3	3422(6)	313(33)	4386(74)	3.4
C4	3420(6)	1418(36)	6069(79)	4.2
C5	2838(5)	959(43)	3598(68)	4.0
C6	2541(6)	966(40)	2673(61)	3.3
C7	1947(6)	434(38)	37(87)	5.4
C8	1953(7)	1465(31)	1546(87)	4.1
C9	1322(7)	806(90)	−2474(138)	14.7
C10	1336(6)	1246(40)	530(105)	6.2
S50	5517(2)	7587(10)	−3594(25)	5.0
S60	4485(2)	4176(9)	3291(25)	4.5
C51	5375(6)	8869(28)	−2263(66)	2.6
C61	4629(6)	3013(24)	5382(72)	2.6
N52	5258(5)	9700(29)	−1495(61)	3.8
N62	4726(5)	2102(33)	6984(62)	4.7

$B_{eq}=4/3(\sum_i\sum_j B_{ij}\ \boldsymbol{a}_i\cdot\boldsymbol{a}_j)$.

+1/2 and +2/3.[8] Considering the charge compensation in the crystal, we can conclude the existence of the magnetic cation, Co^{2+}. In fact the preliminary experiment of SQUID indicates the presence of Co^{2+} and the antiferromagnetic order is observed around 20 K; the magnetic property of α-(BEDT-TTF)$_2$CsCo(SCN)$_4$ will be reported soon.[9] The arrangement of donor is α-type [Fig. 2(b)] and the donor layers and the thick anion sheets stack along the b-axis. In the anion sheet, Co^{2+} is coordinated tetrahedrally by four N atoms and Cs^+ is surrounded by eight S atoms to construct two-dimensional sheet [Fig. 2(c), Table 9].

Table 7. Atomic Coordinates ($\times 10^4$) and Equivalent Isotropic Thermal Parameters of (BEDT-TTF)-$Zn(SCN)_3$

Atom	x	y	z	B_{eq}/Å^2
S1	9366(2)	5872(2)	1273(4)	3.8
S2	8231(2)	6366(2)	−3966(4)	3.2
S3	7197(2)	4581(2)	1465(4)	3.4
S4	6231(2)	4981(2)	−2862(4)	2.9
S5	4983(2)	3008(2)	2155(4)	3.3
S6	3974(2)	3367(2)	−2171(4)	3.1
S7	3101(2)	1494(2)	3205(4)	3.7
S8	1851(2)	1961(2)	−2003(4)	3.5
C1	9970(9)	6686(10)	−725(21)	7.7
C2	9614(8)	6476(10)	−3024(19)	6.3
C3	8036(7)	5425(6)	−30(14)	2.5
C4	7585(6)	5616(6)	−2020(14)	2.3
C5	6072(7)	4328(6)	−497(14)	2.4
C6	5099(7)	3648(6)	−209(14)	2.4
C7	3654(7)	2321(6)	1265(14)	2.6
C8	3168(6)	2504(6)	−666(14)	2.3
C9	1676(7)	1166(7)	2138(16)	3.5
C10	1446(8)	933(7)	−372(16)	3.6
Zn	3113(1)	−1254(1)	−8(2)	3.5
S50	2097(2)	−3461(2)	−6328(5)	4.7
C51	2401(7)	−2751(6)	−4099(16)	3.2
N52	2633(6)	−2269(6)	−2402(14)	4.2
S60	705(2)	−1076(2)	5075(5)	4.6
C61	1461(7)	−1137(6)	−3147(17)	3.2
N62	1994(6)	−1151(6)	1732(14)	4.0
S70	5467(2)	1455(2)	−2637(5)	4.4
C71	4493(7)	545(7)	−1954(17)	3.8
N72	3818(6)	−52(6)	−1391(14)	4.3
H1	982(7)	725(6)	−35(14)	10.2
H2	1069(7)	673(6)	−49(13)	5.4
H3	970(6)	584(6)	−334(14)	9.5
H4	1006(7)	696(6)	−388(13)	6.1
H5	137(7)	65(6)	288(14)	5.1
H6	144(7)	170(6)	251(13)	5.6
H7	69(6)	66(6)	−80(14)	5.3
H8	186(6)	54(6)	−83(14)	7.3

$B_{eq}=4/3(\sum_i\sum_j B_{ij}\ \boldsymbol{a}_i\cdot\boldsymbol{a}_j)$.

In order to understand the molecular interaction, the extended Hückel calculation[10] is carried out for α-(BEDT-TTF)$_2$CsCo(SCN)4. The transverse interaction ($p=-10.6\times10^{-3}$) is much larger than stacking interaction ($c=0.49\times10^{-3}$) and the obtained Fermi surface is closed as shown in Fig. 2(d), which is consistent to the metallic behavior down to 20 K.

For another α-type salt, α-(BEDT-TTF)$Cd_{0.66}$-

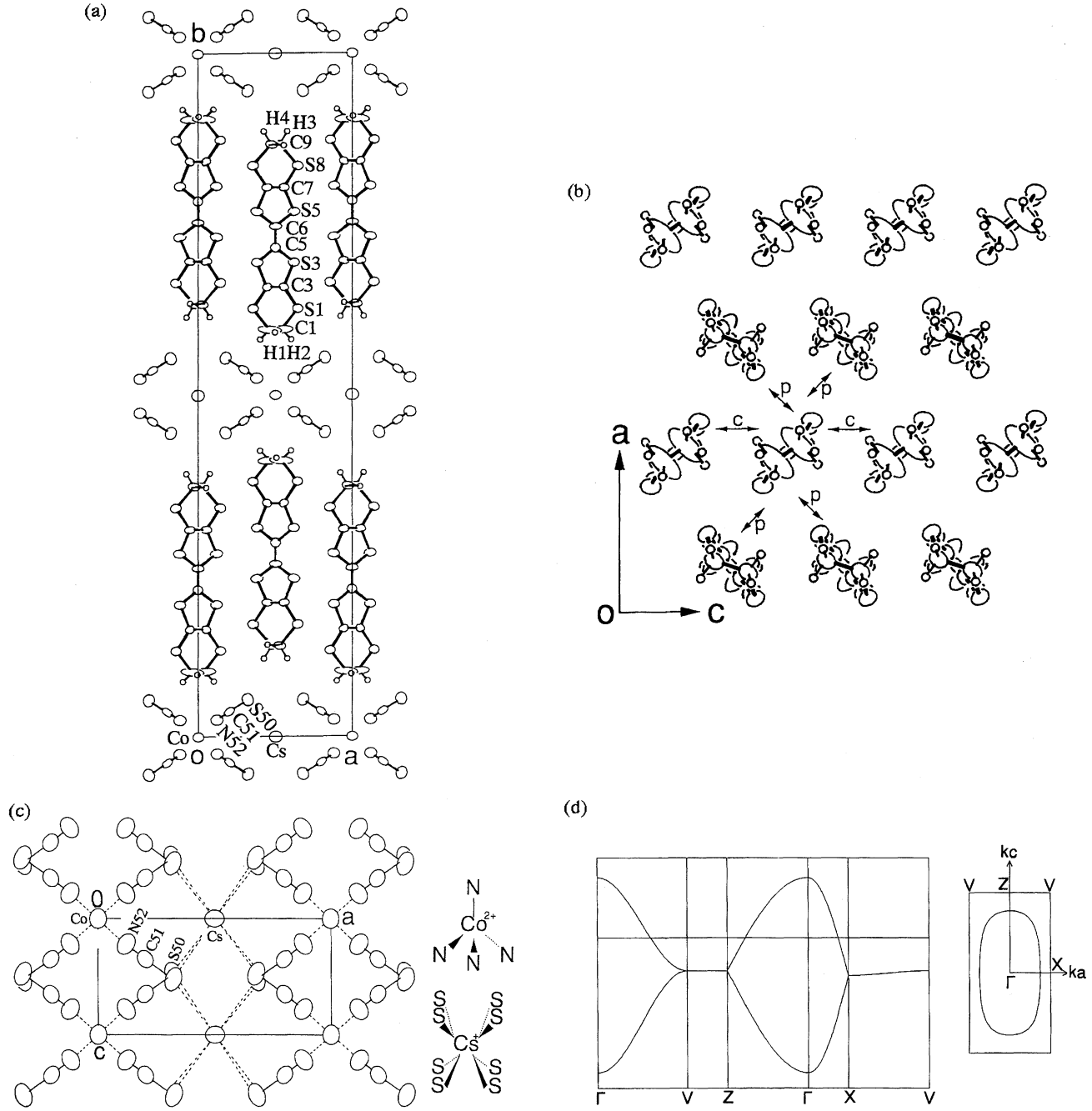

Fig. 2. (a) Crystal structure, (b) donor arrangement, (c) anion arrangement, and (d) band structure of α-(BEDT-TTF)$_2$CsCo(SCN)$_4$. The calculated overlap integrals are $c=0.49$, $p=-10.6$ ($\times 10^{-3}$).

$(SCN)_2$, the existence of Cd and S is confirmed by EDX measurement and the population of Cd^{2+}, 0.66, is determined by the crystal structure analysis. The Cd^{2+} is located on the two-fold axis with probability of 2/3, BEDT-TTF molecule is on an inversion center, and SCN molecule is on a general position. The crystallographically independent molecules are 1/2 of BEDT-TTF, 0.33 of Cd^{2+}, and one SCN. As shown in Fig. 3(a) and Table 10, four S atoms and two N atoms octahedrally coordinate to Cd. The overlap integrals of the donor HOMO on the basis of the extended Hückel calculation are shown in Fig. 3(b) and the band structure based on the tight binding method is depicted in Fig. 3(c). The band is 2/3-filled due to the stoichiometry of α-(BEDT-TTF)$Cd_{0.66}(SCN)_2$. The side-by-side interaction ($p=7.7\times10^{-3}$) is larger than that of the stacking direction ($b=3.5\times10^{-3}$), which is a typical donor arrangement of α-type salts. Since the closed Fermi surface similar to rectangular shape is close to one-dimensional, the nesting of Fermi surface might occur easily. The room temperature conductivity of α-(BEDT-TTF)$Cd_{0.66}(SCN)_2$ is rather high ($\sigma_{RT}=4$ S cm^{-1}), but the semiconducting behavior ($E_a=0.11$ eV) is observed.

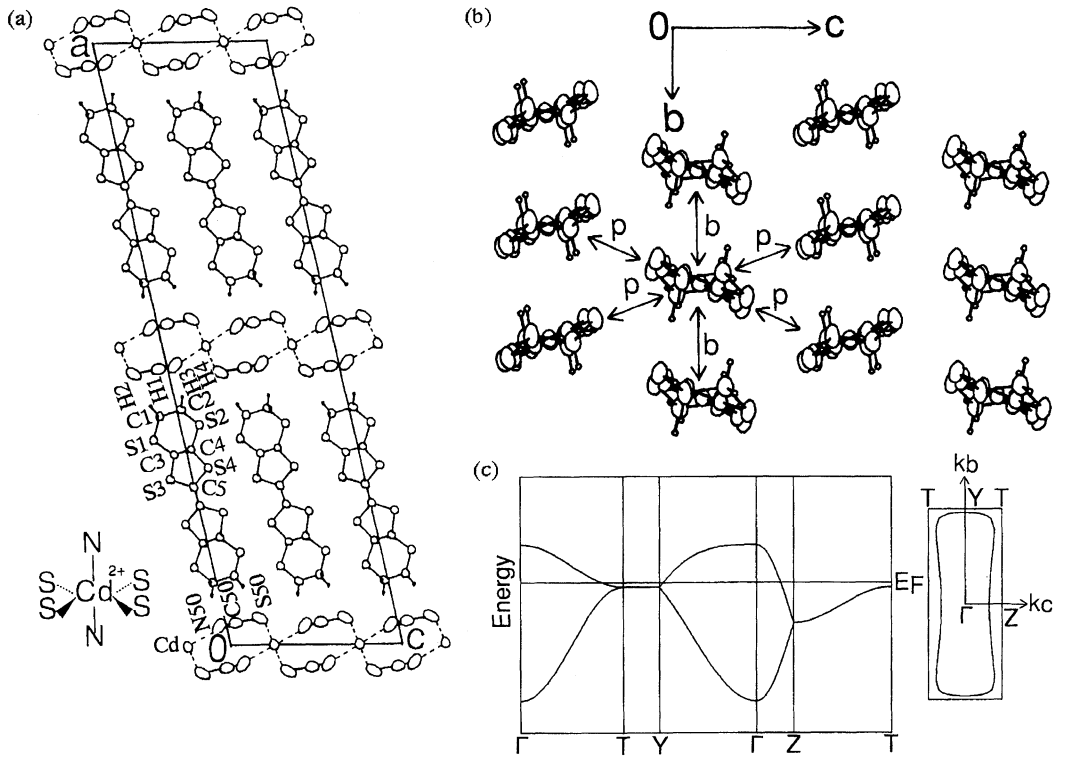

Fig. 3. (a) Crystal structure, (b) donor arrangement, and (c) band structure of α-(BEDT-TTF)$Cd_{0.66}(SCN)_2$. The calculated overlap integrals are b=3.5, p=7.7 ($\times 10^{-3}$).

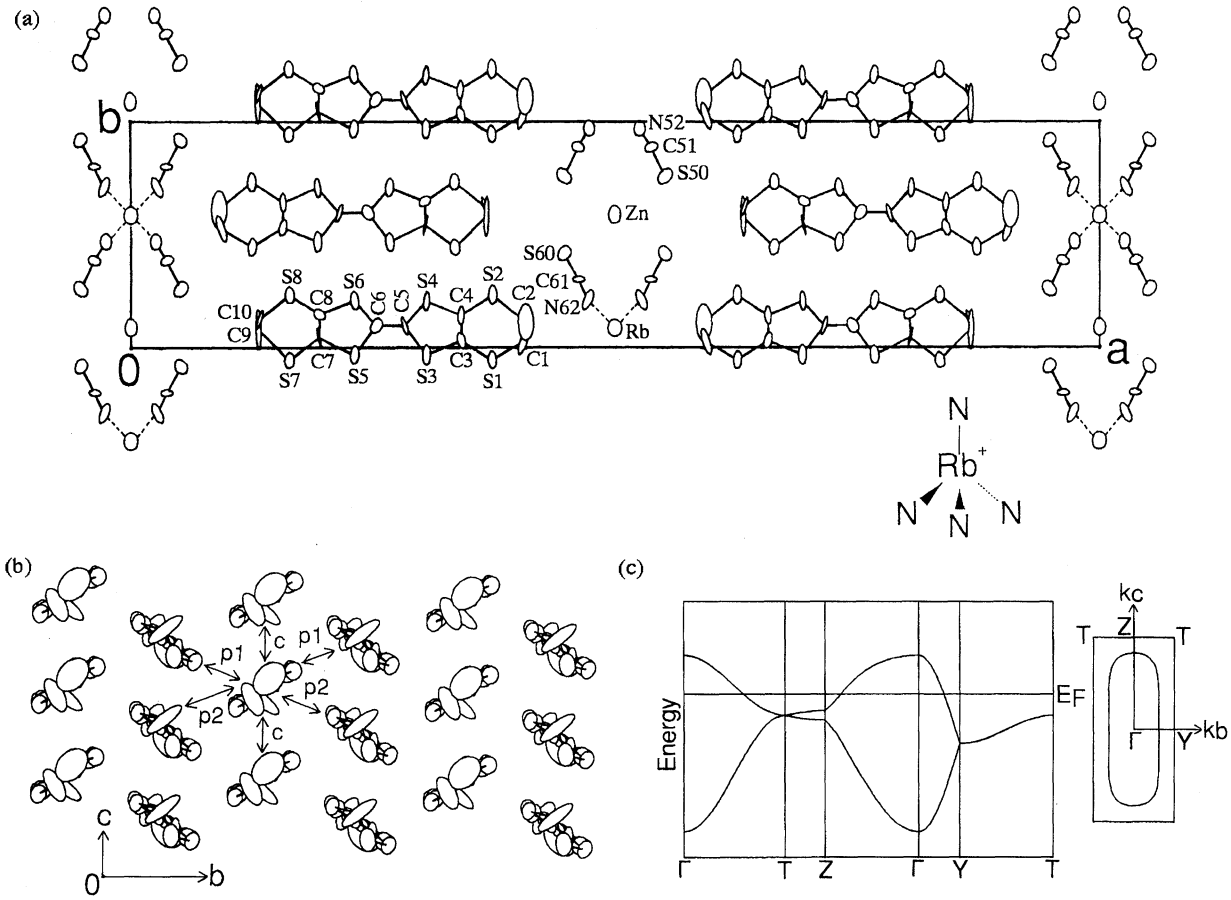

Fig. 4. (a) Crystal structure, (b) donor arrangement, and (c) band structure of α-$(BEDT\text{-}TTF)_2RbZn(SCN)_4$. The calculated overlap integrals are c=2.8, $p1$=8.2, $p2$=9.1 ($\times 10^{-3}$).

Table 8. Atomic Coordinates ($\times 10^4$) and Equivalent Isotropic Thermal Parameters of (BEDT-TTF)$_2$CsCd(SCN)$_4$

Atom	x	y	z	B_{eq}/Å^2
S1	8308(11)	1655(4)	−3797(15)	4.3
S2	10900(10)	1642(4)	1682(14)	4.1
S3	6886(9)	368(4)	−2560(13)	3.1
S4	8969(10)	370(4)	2095(14)	3.3
S5	5108(9)	−1075(4)	−1643(13)	3.1
S6	7140(9)	−1014(4)	3049(13)	2.8
S7	3467(10)	−2423(4)	−1447(13)	3.2
S8	5990(10)	−2350(4)	4207(14)	4.0
C1	10032(39)	2237(14)	−2590(52)	4.4
C2	10373(41)	2327(14)	60(58)	5.6
C3	8362(34)	1068(13)	−1760(45)	3.0
C4	9336(36)	1063(12)	301(46)	3.3
C5	7390(32)	−43(12)	97(44)	2.3
C6	6670(28)	−614(12)	445(41)	1.6
C7	4885(30)	−1783(12)	−70(45)	2.1
C8	5865(29)	−1757(12)	2150(49)	2.4
C9	4054(49)	−3081(15)	285(52)	6.7
C10	4263(40)	−2962(16)	2873(51)	5.3
Cd	0(0)	5000(0)	0(0)	4.2
Cs	5000(0)	5000(0)	5000(0)	4.2
S50	3039(10)	4033(4)	1882(14)	3.5
C51	3758(37)	4226(15)	−342(56)	4.2
N52	4150(31)	4365(12)	−2043(42)	4.4
S60	546(11)	6158(2)	5500(17)	4.8
C61	1983(27)	5804(12)	5179(42)	1.7
N62	3007(25)	5590(11)	4910(41)	3.1

$B_{eq}=4/3(\sum_i\sum_j B_{ij}\ \boldsymbol{a}_i\cdot\boldsymbol{a}_j)$.

Table 9. Intramolecular Bond Lengths (Å) and Angles (°) of α-(et)$_2$CsCo(SCN)$_4$ and α-(et)$_2$CsZn(SCN)$_4$ (M′=Co or Zn)

	α-(et)$_2$CsCo(SCN)$_4$	α-(et)$_2$CsZn(SCN)$_4$
M′–N52	1.92(1)	1.95(4)
Cs–S50	3.895(5)	3.92(2)
Cs–S50[a]	3.747(5)	3.74(2)
S50–C51	1.63(1)	1.66(5)
C51–N52	1.15(1)	1.12(5)
S1–C1	1.79(2)	1.82(5)
S1–C3	1.744(9)	1.74(4)
S3–C3	1.761(9)	1.80(4)
S3–C5	1.748(7)	1.67(3)
S5–C6	1.732(6)	1.79(4)
S5–C7	1.736(9)	1.65(5)
S7–C7	1.750(9)	1.81(5)
S7–C9	1.81(1)	1.74(5)
C1–C1[b]	1.21(5)	1.3(1)
C3–C3[b]	1.35(2)	1.39(7)
C5–C6	1.37(1)	1.40(7)
C7–C7[b]	1.35(2)	1.33(8)
C9–C9[b]	1.55(3)	1.57(9)
N52–M′-N52[c]	112.5(6)	110(2)
N52–M′-N52[d]	104.5(6)	108(2)
S50–Cs–S50[d]	126.8(1)	126.6(4)
S50–Cs–S50[e]	79.20(7)	78.9(3)
S50–Cs–S50[a]	76.72(8)	76.7(3)
S50–Cs–S50[f]	98.1(2)	97.9(6)
S50–Cs–S50[b]	54.42(9)	54.8(4)
S50–C51–N52	178(1)	177(4)

a) $x, -y, 1-z$; b) $1-x, y, 1-z$; c) $-x, -y, z$; d) $x, -y, -z$; e) $x, y, z-1$; f) $1-x, -y, z$.

Table 10. Intramolecular Bond Lengths (Å) and Angles (°) of α-(et)Cd$_{0.66}$(SCN)$_2$

Cd–S50[a]	2.918(7)
Cd–S50[b]	2.973(7)
Cd–N50	2.45(1)
S50–C50	1.68(1)
C50–N50	1.14(2)
S1–C1	1.814(9)
S1–C3	1.764(8)
S2–C2	1.82(1)
S2–C4	1.765(7)
S3–C3	1.738(7)
S3–C5	1.753(9)
S4–C4	1.747(8)
S4–C5	1.752(7)
C1–C2	1.51(1)
C3–C4	1.33(1)
C5–C5[c]	1.33(1)
S50–C50–N50	178(1)

a) $x, -y, z-0.5$; b) $x, -y+1, z-0.5$; c) $-x+0.5, -y+0.5, -z$.

Table 11. Intramolecular Bond Lengths (Å) and Angles (°) of α-(et)$_2$RbZn(SCN)$_4$

Zn–S50	3.71(1)	S5–C6	1.84(4)
Zn–S50[a]	3.62(1)	S5–C7	1.83(4)
Zn–S60	3.71(1)	S6–C6	1.69(4)
Zn–S60[a]	3.61(1)	S6–C8	1.77(4)
Rb–N52[b]	1.94(3)	S7–C7	1.77(4)
Rb–N52[c]	1.93	S7–C9	1.98(9)
Rb–N62[d]	2.01(3)	S8–C8	1.73(4)
Rb–N62[e]	2.01	S8–C10	1.75(5)
S50–C51	1.66(3)	C1–C2	1.38(2)
C51–N52	1.12(4)	C3–C4	1.37(5)
S60–C61	1.55(4)	C5–C6	1.29(6)
C61–N62	1.19(5)	C7–C8	1.26(6)
S1–C1	1.70(7)	C9–C10	1.4(1)
S1–C3	1.72(4)		
S2–C2	2.0(1)	S50–Zn–S50[a]	124.3
S2–C4	1.79(4)	S50–Zn–S60[a]	56.7
S3–C3	1.73(4)	N52[b]–Rb–N52[c]	105.1
S3–C5	1.84(5)	N52[b]–Rb–N62[d]	116.5
S4–C4	1.74(4)	N62[d]–Rb–N62[e]	101.9
S4–C5	1.69(5)	S60–Zn–S60[a]	122.4

a) $1-x, y, -z$; b) $x, y-1, z$; c) $1-x, y-1, -z$ d) $x, y, z-1$; e) $1-x, y, -z+1$.

Figure 4(a) depicts the crystal structure of α-(BEDT-TTF)$_2$RbZn(SCN)$_4$. The Rb^+ and Zn^{2+} are allocated on the two-fold axis and the BEDT-TTF and two SCN molecules are on a general position. Therefore the crystallographically independent molecules are 1/2 of Rb^+ and Zn^{2+}, one BEDT-TTF, and two SCN. In the anion layer, four N atoms are connected to Rb^+ tetrahedrally. Though the distances of $Zn^{2+}\cdots$S are 3.61—3.71 Å that is longer than ionic and van der Waals radii sum, $r(Zn^{2+})+r(S)=0.74+1.8=2.54$ Å,[1] Zn^{2+} is surrounded

by four S atoms to form square plane (Table 11). The donor arrangement is another α-type with the space group C2. It is characteristic of α-phase that the calculated overlap integrals between donor columns, $p1$ (8.2×10^{-3}) and $p2$ (9.1×10^{-3}), are 3—4 times as large as that within the column, c (2.8×10^{-3}) (Fig. 4(b)). The band structure (Fig. 4(c)) is calculated; the Fermi surface is closed and has rectangular-like shape. The resistivity of α-(BEDT-TTF)$_2$RbZn(SCN)$_4$ is metallic down to 180 K, but the sample is cracked at that temperature due to brittleness of the crystal.

As shown in Table 1, the resistivity of (BEDT-TTF)-Zn(SCN)$_3$ is comparatively high ($\rho_{RT}=180\ \Omega$cm, $E_a=0.18$ eV) because of the +1 charge on BEDT-TTF with 1/2 filled band. The +1 charge of donor can be easily concluded from the anion charge, $[Zn(SCN)_3]^-$. The crystallographically independent molecules are one BEDT-TTF and Zn(SCN)$_3$ which are on the general position. The distances of central C=C and average C–S on BEDT-TTF molecule are 1.39(1) and 1.719 Å, which indicates +1 charge of BEDT-TTF[8] (Table 12). The donor (D) and $[Zn_2(SCN)_6]^{2-}$ (A) form mixed-stacked structure like DDADDA as shown in Fig. 5. Three N atoms and a S atom are tetrahedrally coordinated to Zn^{2+} to form a $[Zn_2(SCN)_6]^{2-}$ cluster.

Figure 6 shows the crystal structure of (BEDT-TTF)$_2$CsCd(SCN)$_4$. The Cs^+ and Cd^{2+} are on inversion centers and BEDT-TTF and SCN molecules are allocated on general positions. Therefore crystallographically independent molecules are 1/2 of Cs^+ and Cd^{2+}, one BEDT-TTF, and two SCN. Cs^+ is coordinated by four N atoms to form a square-plane. The distances of Cd-S50, Cd-S60[a], and Cd-N62 are 3.638(9), 3.62(1), and 3.50(2) Å which are larger than ionic and van der Waals radii sum, $r(Cd^{2+})+r(S)=1.09+1.8=2.89$ and $r(Cd^{2+})+r(N)=1.09+1.55=2.64$ Å[1] (Table 13). The donor arrangement of (BEDT-TTF)$_2$CsCd(SCN)$_4$ is not the α-type, but similar to that of (BEDT-TTF)$_3$(ClO$_4$)$_2$[11] (Fig. 6(b)). The semiconducting behavior ($E_a=0.02$ eV) is observed with the rather high room conductivity of 10 S cm^{-1}.

In conclusion, we prepared new three-component organic conductor, (BEDT-TTF)$_2$MM′(SCN)$_4$ [M=K, Rb, Cs; M′=Co, Zn, Cd]. The crystal structure analyses indicate that three-component system afford the

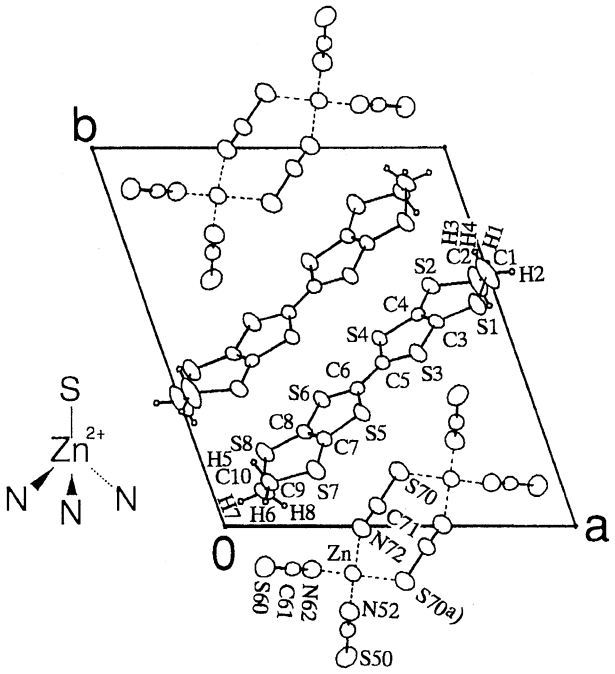

Fig. 5. Crystal structure of (BEDT-TTF)Zn(SCN)$_3$.

Table 12. Intramolecular Bond Lengths (Å) and Angles (°) of (et)Zn(SCN)$_3$

Zn–S70[a]	2.411(3)	S6–C6	1.707(8)
Zn–N52	1.942(8)	S6–C8	1.740(8)
Zn–N62	1.935(9)	S7–C7	1.766(9)
Zn–N72	2.006(8)	S7–C9	1.816(9)
S50–C51	1.60(1)	S8–C8	1.747(8)
C51–N52	1.17(1)	S8–C10	1.82(1)
S60–C61	1.62(1)	C1–C2	1.38(2)
C61–N62	1.16(1)	C3–C4	1.34(1)
S70–C71	1.651(9)	C5–C6	1.39(1)
C71–N72	1.13(1)	C7–C8	1.33(1)
S1–C1	1.80(1)		
S1–C3	1.742(8)		
S2–C2	1.80(1)	N52–Zn–N62	114.4(3)
S2–C4	1.741(9)	N62–Zn–N72	111.6(4)
S3–C3	1.741(8)	N72–Zn–S70[a]	104.4
S3–C5	1.710(8)	S70[a]–Zn–N52	110.1
S4–C4	1.741(8)	S50–C51–N52	176(1)
S4–C5	1.736(9)	S60–C61–N62	177(1)
S5–C6	1.724(9)	S70–C71–N72	176(1)
S5–C7	1.738(8)		

a) $1-x, -y, -z$.

Table 13. Intramolecular Bond Lengths (Å) and Angles (°) of (et)$_2$CsCd(SCN)$_4$

Cd–S50	3.638(9)	S7–C9	1.79(3)
Cd–S60[a]	3.62(1)	S8–C8	1.72(3)
Cd–N62	3.50(2)	S8–C10	1.85(3)
Cs–N52	2.36(3)	C1–C2	1.50(4)
Cs–N62	2.33(2)	C3–C4	1.31(4)
S1–C1	1.80(3)	C5–C6	1.29(3)
S1–C3	1.71(3)	C7–C8	1.38(3)
S2–C2	1.79(3)	C9–C10	1.48(4)
S2–C4	1.73(3)	S50–C51	1.59(4)
S3–C3	1.78(3)	C51–N52	1.14(4)
S3–C5	1.77(3)	S60–C61	1.63(4)
S4–C4	1.81(3)	C61–N62	1.13(4)
S4–C5	1.71(2)		
S5–C6	1.77(2)		
S5–C7	1.75(3)	N52–Cs–N62	89(1)
S6–C6	1.73(2)	S50–C51–N52	174(3)
S6–C8	1.76(2)	S60–C61–N62	176(2)
S7–C7	1.73(2)		

a) $x, y, z-1$.

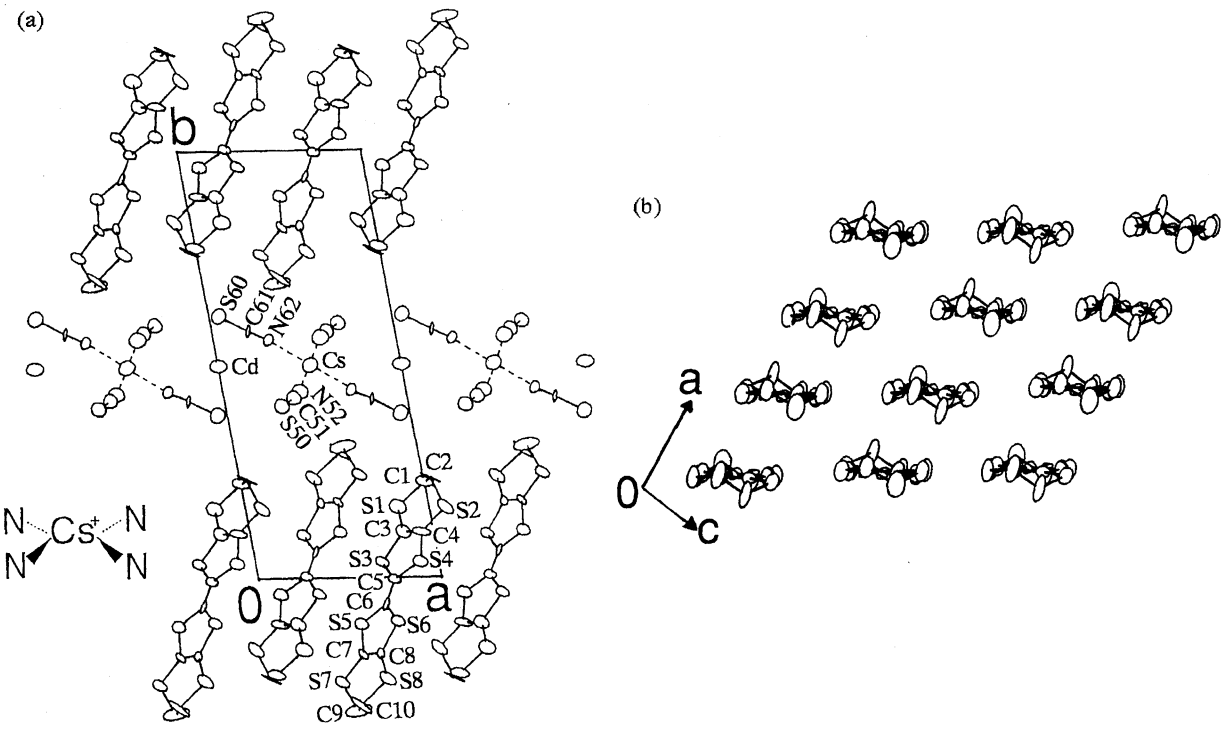

Fig. 6. (a) Crystal structure and (b) donor arrangement of $(BEDT\text{-}TTF)_2CsCd(SCN)_4$.

α-type donor arrangement like α-$(BEDT\text{-}TTF)_2CsCo(SCN)_4$, α-$(BEDT\text{-}TTF)_2RbZn(SCN)_4$, α-$(BEDT\text{-}TTF)_2CsZn(SCN)_4$, and α-$(BEDT\text{-}TTF)Cd_{0.66}(SCN)_2$ except ClO_4-type of $(BEDT\text{-}TTF)_2CsCd(SCN)_4$. The first three salts show metallic behavior and especially $(BEDT\text{-}TTF)_2CsM'(SCN)_4$ exhibits a metal-insulator transition at 20 K at ambient pressure. In the pressurized condition of 5 kbar, semiconducting behavior was obtained for α-$(BEDT\text{-}TTF)_2CsZn(SCN)_4$. Since α-$(BEDT\text{-}TTF)_2CsCo(SCN)_4$ contains magnetic cation, Co^{2+}, it is interesting to investigate whether there is an interaction between itinerant spin of $BEDT\text{-}TTF^+$ and localized spin of Co^{2+} or not.

References

1) "Handbook of Chemistry and Physics," CRC Press, Vol. 70, F-187 (1989); R. D. Shannon, *Acta Crystallogr., Sect. A*, **A32**, 751 (1976); A. Bondi, *J. Phys. Chem.*, **68**, 441 (1964).

2) a) M. Oshima, H. Mori, G. Saito, and K. Oshima, *Chem. Lett.*, **1989**, 1159; b) H. Mori, S. Tanaka, M. Oshima, G. Saito, T. Mori, Y. Maruyama, and H. Inokuchi, *Bull. Chem. Soc. Jpn.*, **63**, 2183 (1990); c) H. Mori, S. Tanaka, K. Oshima, M. Oshima, G. Saito, T. Mori, Y. Maruyama, and H. Inokuchi, *Solid State Commun.*, **74**, 1261 (1990); d) H. Mori, S. Tanaka, K. Oshima, G. Saito, T. Mori, Y. Maruyama, and H. Inokuchi, *Synth. Met.*, **41—43**, 2013 (1991); e) H. Mori, S. Tanaka, T. Mori, Y. Maruyama, H. Inokuchi, and G. Saito, *Solid State Commun.*, **78**, 49 (1991); f) H. Mori, I. Hirabayashi, S. Tanaka, T. Mori, Y. Maruyama, H. Inokuchi, and G. Saito, *Synth. Met.*, **55—57**, 2443 (1993); g) N. D. Kushch, L. I. Buravov, M. V. Kartsovnik, V. N. Laukhin, S. I. Pesotskii, R. P. Shibaeva, L. P. Rosenberg, E. B. Yagubskii, and A. V. Zvarykina, *Synth. Met.*, **46**, 271 (1992).

3) T. Sasaki and N. Toyota, *Synth. Met.*, **55—57**, 2296 (1993).

4) H. H. Wang, K. D. Carlson, U. Geiser, W. K. Kwok, M. D. Vashon, J. E. Thompson, N. F. Larsen, G. D. McCabe, R. S. Hulscher, and J. M. Williams, *Physica B+C (Amsterdm)*, **166 B+C**, 57 (1990).

5) H. Mori et al., to be submitted.

6) G. M. Sheldrick, "Crystallographic Computing 3," Oxford University Press, Oxford (1985), pp. 175—189.

7) T. Mori, private communication.

8) H. Kobayashi, R. Kato, T. Mori, A. Kobayashi, Y. Sasaki, G. Saito, T. Enoki, and H. Inokuchi, *Mol. Cryst. Liq. Cryst.*, **107**, 33 (1984).

9) H. Mori et al., to be submitted.

10) T. Mori, A. Kobayashi, T. Sasaki, H. Kobayashi, G. Saito, and H. Inokuchi, *Bull. Chem. Soc. Jpn.*, **57**, 627 (1984).

11) H. Kobayashi, A. Kobayashi, Y. Sasaki, G. Saito, T. Enoki, and H. Inokuchi, *Chem. Lett.*, **1984**, 179.